Observation of optical precursors at the biphoton level

Shengwang Du,[1,2,*] Chinmay Belthangady,[1] Pavel Kolchin,[1] G. Y. Yin,[1] and S. E. Harris[1]

[1]*Edward L. Ginzton Laboratory, Stanford University, Stanford, California 94305, USA*
[2]*Present address: Department of Physics, The Hong Kong University of Science and Technology, Clear Water Bay, Kowloon, Hong Kong, China*
**Corresponding author: dusw@ust.hk*

Received June 25, 2008; revised July 27, 2008; accepted August 11, 2008; posted August 18, 2008 (Doc. ID 97726); published September 12, 2008

We describe the observation of a sharp leading-edge spike in a biphoton wave packet that is produced using slow light and measured by two-photon correlation. Using the stationary-phase approximation we characterize this spike as a Sommerfeld–Brillouin precursor resulting from the interference of low- and high-frequency spectral components. © 2008 Optical Society of America

OCIS codes: 270.0270, 070.7345.

Optical precursors were first described by Sommerfeld and Brillouin in 1907 and are of importance in electromagnetic theory because they ensure that the front edge of a wave packet will always travel at the velocity of light in vacuum. It was previously believed that optical precursors existed for only a few optical cycles and contributed little to the amplitude of the field [1]. However, recent theoretical [2] and experimental [3] work has shown that in a narrow-resonance atomic medium the precursor magnitude can be of the same order as the primary field, and its length may be much longer than a few cycles. Precursors have been extensively studied in the gamma ray [4], microwave [5], and optical regimes [3,6–9].

In this Letter, we extend the classical concept of precursors to describe the behavior of biphoton wave-packets that are measured by correlation using single-photon-counting modules (SPCMs). The measured wave packets are generated by using electromagnetically induced transparency (EIT) and slow light [10,11] so that the correlation time of the main body of the wave packet can be varied over the range of 50–900 ns [12]. We remark that the observation of the sharp leading edge spike in [12] was not expected, and its nature was first suggested to us by Daniel J. Gauthier. A requirement for the sharp front-edge spike to be apparent is that the optical depth (OD) be sufficiently large so that the pulse length is determined by the group delay.

A schematic of biphoton generation is shown in Fig. 1. In the presence of counterpropagating cw pump (ω_p) and coupling (ω_c) lasers, phase-matched, paired Stokes (ω_s) and anti-Stokes (ω_{as}) photons are spontaneously generated and propagate in opposite directions. We use a 2D ^{85}Rb magneto-optical trap (MOT) with a longitudinal length $L=1.7$ cm and an aspect ratio of 25. The Stokes (σ^-) and anti-Stokes (σ^+) photons are coupled into opposing single-mode fibers and detected by two SPCMs after passage through two narrowband optical filters (F1 and F2). With the dephasing rate of the $|1\rangle \rightarrow |3\rangle$ transition denoted by $\gamma_{13}=2\pi\times 3\times 10^6 \text{sec}^{-1}$, the pump laser has a Rabi frequency of $\Omega_p=1.16\gamma_{13}$, is σ^- circularly polarized, and is blue detuned from the $|1\rangle \rightarrow |4\rangle$ transition by $\Delta_p=48.67\gamma_{13}$. The coupling laser ($\Omega_c$) is σ^+ circularly polarized and is on resonance with the $|2\rangle \rightarrow |3\rangle$ transition. Further experimental details are described in [12].

We first note that the Glauber correlation function, or equivalently the coincidence rate versus the relative time delay τ, for an ideal parametric down converter with a frequency independent group delay between the signal and the idler of L/V_g is a rectangle [Fig. 2(a)]. Each biphoton (pair of photons) is emitted at a random position; if the point of emission is at the front edge of the nonlinear medium, then the photons arrive simultaneously; if it is at the back edge, then one is delayed from the other by L/V_g. For an EIT-based downconverter operating at high optical depth, the anti-Stokes photon travels slowly, and because the bandwidth is constrained by the EIT profile, the correlation profile is smoothed and has a full width equal to the group delay. Figure 2(b) shows the experimentally observed correlation function with a correlation width of about 400 ns, as compared to the measured group delay of $L/V_g=372$ ns. It is the sharp peak and the oscillatory structure at the leading edge that require further explanation.

The experimental curve, including the leading edge, is in good agreement with the Heisenberg picture theory of earlier papers from our group [12–14]. To explicitly display the phase of the biphoton, we start here with the equivalent Schrödinger picture wave function. With the assumption that the off-resonant pumping laser is sufficiently weak that the

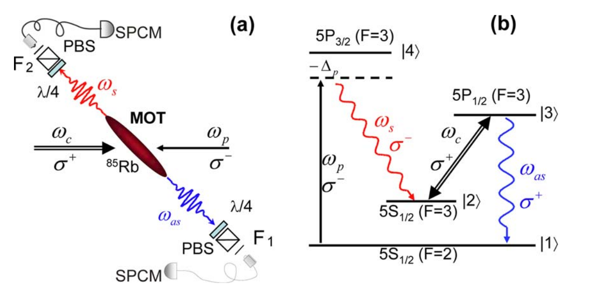

Fig. 1. (Color online) Biphoton generation in a double-Λ system. (a) Experimental configuration. (b) ^{85}Rb energy level diagram (from [12]).

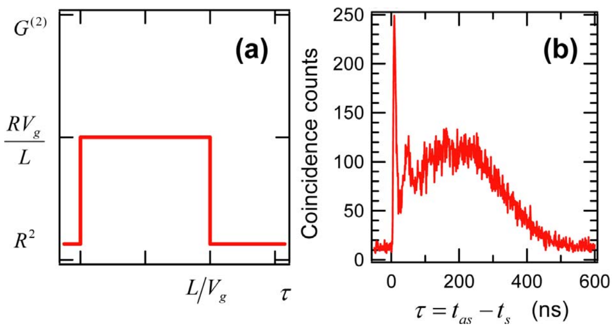

Fig. 2. (Color online) (a) Two-photon correlation for an ideal spontaneous parametric down converter with a relative group delay L/V_g and paired emission rate R. (b) Experimental Stokes–anti-Stokes coincidence counts per 1 ns bin in 800 s as a function of delay at an optical depth of 62, $\Omega_c = 4.20\gamma_{13}$, $\Omega_p = 1.16\gamma_{13}$, and $\Delta_p = 48.67\gamma_{13}$.

atomic population remains primarily in the ground level $|1\rangle$, and $\tau = t_{as} - t_s$, the two-time Stokes–anti-Stokes biphoton wave function is $\Psi(t_s, t_s + \tau) = \psi(\tau)e^{-i(\omega_c+\omega_p)t_s}$, where the envelope quantity is [15–17]

$$\psi(\tau) = \frac{L}{2\pi}\int \kappa(\omega)\varphi(\omega)e^{i\theta(\omega,\tau)}\mathrm{d}\omega. \qquad (1)$$

Here the quantity ω denotes the anti-Stokes frequency, $\kappa(\omega)$ is the nonlinear coupling coefficient, and $\theta(\omega,\tau) = \mathrm{Re}[(k_{as}+k_s)L/2 - \omega\tau]$ is the real phase function. $k_{as}(\omega)$ and $k_s(\omega)$ are the complex angular wavenumbers. With $\Delta k(\omega) = (\vec{k}_{as} + \vec{k}_s^* - \vec{k}_c - \vec{k}_p)\cdot\vec{z}$, and the unit vector $\vec{z}$ taken in the direction of anti-Stokes generation, $\varphi(\omega) = \mathrm{sinc}(\Delta k L/2)\exp\{-\mathrm{Im}[(k_{as}+k_s)L/2]\}$. Expressions for these quantities in terms of the pertinent susceptibilities are given in [17]. The two-photon Glauber correlation function can be expressed in terms of the biphoton wave function as $G^{(2)}(\tau) = |\psi(\tau)|^2 + B$, where the background B results from uncorrelated photons.

As is the case for propagating classical wave packets, the method of stationary phase may be used to explain the biphoton precursor. The essential idea is that the dominant contribution to the integral in Eq. (1) occurs when the derivative of $\theta(\omega,\tau)$ is equal to zero [18]. For different frequencies this zero occurs at different times τ. By differentiating $\theta(\omega,\tau)$ we see that the relative delay time τ is related to the dominant frequency ω_d by

$$\tau = \frac{L}{2V_g(\omega_d)} - \frac{L}{2c}, \qquad (2)$$

where we have taken $k_s = (\omega_c + \omega_p - \omega)/c$.

The upper and lower portions of Fig. 3 show the measured EIT transmission and the calculated right-hand side of Eq. (2) as functions of anti-Stokes frequency detuning $\Delta\omega = \omega - \omega_{13}$ from $|1\rangle \to |3\rangle$ transition, respectively. Though it is not apparent in this figure, the right-side asymptote approaches zero faster than the left asymptote does. Therefore the earliest portion of the biphoton wave packet to intersect with the

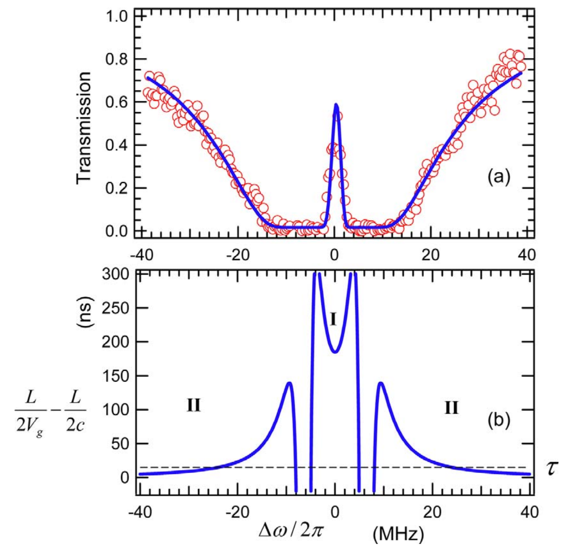

Fig. 3. (Color online) (a) Anti-Stokes (EIT) transmission profile. (b) Group delay $L/2V_g$ as a function of anti-Stokes detuning $\Delta\omega$. Optical depth=62, $\Omega_c = 4.20\gamma_{13}$.

horizontal line τ and to arrive at the detector comes from the high-frequency portion of the spectrum and is thought of as the Sommerfeld precursor. At slightly later times the low-frequency Brillouin components arrive at the detector and beat with the simultaneously arriving high-frequency components.

We may think of $\psi(\tau)$ in Eq. (1) as having two portions that arise from different regions in frequency space, i.e.,

$$\psi(\tau) = \psi_0(\tau) + \psi_{SB}(\tau). \qquad (3)$$

The function $\psi_0(\tau)$ is the main body of the biphoton and contains most of its energy. It is obtained by numerically integrating over the central region I of Fig. 3 that extends $\Delta\omega$ from $-\Omega_c/2$ to $\Omega_c/2$:

$$\psi_0(\tau) = \frac{L}{2\pi}\int_{\omega_{13}-\Omega_c/2}^{\omega_{13}+\Omega_c/2} \kappa(\omega)\varphi(\omega)e^{i\theta(\omega,\tau)}\mathrm{d}\omega. \qquad (4)$$

The function $\psi_{SB}(\tau)$ is the Sommerfeld–Brillouin precursor and is obtained by integrating over region II of Fig. 3. For an oscillatory integral of the form $f = \int_{-\infty}^{\infty}F(\omega)e^{i\theta(\omega)}\mathrm{d}\omega$, where $F(\omega)$ varies slowly as compared to the real phase $\theta(\omega)$, the dominant contribution to the integral occurs when the derivative, $\theta'(\omega_d)$ is equal to zero. We expand $\theta(\omega) \simeq \theta(\omega_d) + \frac{1}{2}\theta''(\omega_d)(\omega - \omega_d)^2$ and integrate over ω. With the contribution of the end points neglected, this integral is $f_d = \sqrt{2\pi i/\theta''(\omega_d)}F(\omega_d)e^{i\theta(\omega_d)}$. When there are several points of stationary phase, it follows that the Sommerfeld–Brillouin portion of the wave packet is [18]

$$\psi_{SB}(\tau) = \sum_{\omega_d} \frac{\kappa(\omega_d)\varphi(\omega_d)L}{\sqrt{-i2\pi\theta''(\omega_d)}}e^{i\theta(\omega_d,\tau)}. \qquad (5)$$

Figure 4 is a zoomed view of Fig. 2(b) from 0 to 125 ns. The theoretical curve is obtained from Eqs. (3)–(5) with a vertical scaling factor to best

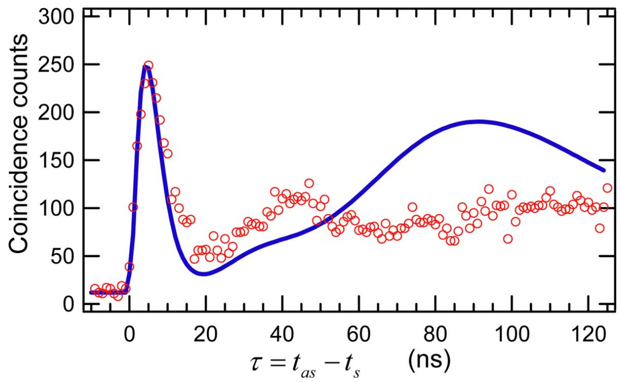

Fig. 4. (Color online) Zoomed view of Fig. 2(b) comparing the experimental data (circles) and the theoretical curve (solid curve). Optical depth=62.

fit the experimental data. The leading-edge Sommerfeld–Brillouin precursor has a width of about 10 ns. Experimental and theoretical results at smaller OD (30 and 53) and different Ω_c are plotted in Fig. 5. All show reasonable agreement between Eq. (1), or equivalently Eqs. (3)–(5) and the experiment.

The width at half power of the precursor as determined by evaluating Eq. (5) is 7 ns at an optical depth of 62. A still coarser estimate is obtained by taking the functional form of the beating as $\cos^2(\Delta\omega_d \tau)$ with the width at half power occuring when $\Delta\omega_d \tau = \pi/4$ and the line shape as Lorentzian. The group delay at a detuning $\Delta\omega$ in the wing of a naturally broadened Lorentzian line may be expressed in terms of the Einstein A coefficient and the optical depth $N\sigma L$ as $L/V_g = AN\sigma L/(4\Delta\omega^2)$, where N is atomic density and σ is the anti-Stokes on-resonance absorption cross section. Combining these expressions, the half-power width of the precursor spike is $\pi^2/(AN\sigma L)$. At an optical depth of 62 as in Fig. 4 and a natural decay time of 26.5 ns ($A = 2\gamma_{13}$), this formula predicts a precursor width of 4.2 ns.

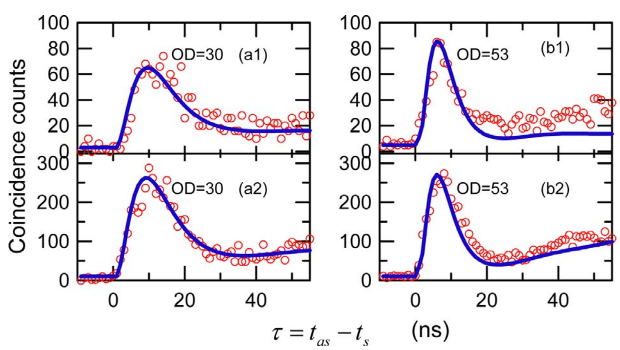

Fig. 5. (Color online) Comparison of theory and experiment for other parameters. In parts (a1) and (b1) $\Omega_c = 2.35\gamma_{13}$. In parts (a2) and (b2) $\Omega_c = 4.20\gamma_{13}$.

It might be hypothesized that the observed shape is not a Sommerfeld–Brillouin precursor but instead results from the high optical depth and nonzero loss experienced by the anti-Stokes field. To test this we have used Eq. (1) and also the exact operator equations with, in both cases, the spontaneous decay rate and both dephasing rates set to zero, thereby creating a lossless system. We find that except for a slightly more pronounced oscillation, the precursor has the same shape as in Figs. 4 and 5. We have thereby verified that the Sommerfeld–Brillouin precursor is dominantly the result of the interplay of phases during nominally lossless propagation.

The authors thank D. J. Gauthier, J. -M. Wen, and H. Jeong for helpful discussions. The work was supported by the Defense Advanced Research Projects Agency (DARPA), the U.S. Air Force Office of Scientific Research (USAFOSR), and the U.S. Army Research Office (USARO).

References

1. L. Brillouin, *Wave Propagation and Group Velocity* (Academic, 1960).
2. W. R. LeFew, S. Venakides, and D. J. Gauthier, arXiv:0705.4238 [physics.optics].
3. H. Jeong, A. M. C. Dawes, and D. J. Gauthier, Phys. Rev. Lett. **96**, 143901 (2006).
4. F. J. Lynch, R. E. Holland, and M. Hamermesh, Phys. Rev. **120**, 513 (1960).
5. P. Pleshko and I. Palocz, Phys. Rev. Lett. **22**, 1201 (1969).
6. J. Aavikscoo, J. Lippmaa, and J. Kuhl, J. Opt. Soc. Am. B **5**, 1631 (1988).
7. J. Aavikscoo, J. Kuhl, and K. Ploog, Phys. Rev. A **44**, R5353 (1991).
8. S.-H. Choi and U. L. Österberg, Phys. Rev. Lett. **92**, 193903 (2004).
9. H. Jeong and U. L. Österberg, Phys. Rev. A **77**, 021803(R) (2008).
10. S. E. Harris, Phys. Today **50**, 36 (1997).
11. M. Fleischhauer, A. Imamoglu, and J. P. Marangos, Rev. Mod. Phys. **77**, 633 (2005).
12. S. Du, P. Kolchin, C. Belthangady, G. Y. Yin, and S. E. Harris, Phys. Rev. Lett. **100**, 183603 (2008).
13. V. Balić, D. A. Braje, P. Kolchin, G. Y. Yin, and S. E. Harris, Phys. Rev. Lett. **94**, 183601 (2005).
14. P. Kolchin, Phys. Rev. A **75**, 033814 (2007).
15. M. H. Rubin, D. N. Klyshko, Y. H. Shih, and A. V. Sergienko, Phys. Rev. A **50**, 5122 (1994).
16. S. Du, E. Oh, J.-M. Wen, and M. H. Rubin, Phys. Rev. A **76**, 013803 (2007).
17. S. Du, J.-M. Wen, and M. H. Rubin, "Narrowband biphoton generation near atomic resonance," J. Opt. Soc. Am. B (to be published).
18. J. D. Jackson, *Classical Electrodynamics*, 2nd ed. (Wiley, 1975).